

Neural Modeling and Control of a ^{13}C Isotope Separation Process

Vlad Muresan¹, Mihail Abrudean¹, Honoriu Valean¹, Tiberiu Colosi¹, Mihaela-Ligia Ungureșan²,
Valentin Sita¹, Iulia Clitan¹ and Daniel Moga¹

¹Automation Department, Technical University of Cluj-Napoca, Barițiu Street, Cluj-Napoca, Romania

²Physics and Chemistry Department, Technical University of Cluj-Napoca, Barițiu Street, Cluj-Napoca, Romania

Keywords: Separation Column, ^{13}C Isotope, Internal Model Control Strategy, Neural Networks, Distributed Parameter Process, Approximating Analytical Solution.

Abstract: The paper presents a solution for the ^{13}C isotope concentration control inside and at the output of a separation column, solution based on the Internal Model Control strategy. The ^{13}C isotope results from a chemical exchange process carbon dioxide – carbamate, which is a distributed parameter process. In order to model the mentioned process, an original form of the approximating analytical solution which describes the process work in transitory regime is determined. The evolution of the approximating solution depends both on time and on the position from the column height. The reference model of the fixed part of the control structure is implemented using neural networks, representing an original solution due to the fact that a neural model is determined for a distributed parameter process. The controller is, also, implemented using neural networks, its main parameter being adapted in relation to the transducer position change in the separation column. The advantages of using the proposed concentration control strategy consist of: the possibility of controlling the value of the ^{13}C isotope concentration in any point from the separation column height; the improvement of the system performance regarding the settling time; the possibility to reject the effect of the disturbances.

1 INTRODUCTION

The plant used for the separation of the ^{13}C isotope is presented in Figure 1. The absorber A is supplied with ethanolamine using the pump P through the pipe 1 and with carbon dioxide (CO_2) at approximately 99.98% concentration through the pipe 5. In A the absorption (Dang and Rochelle, 2003; Dugas and Rochelle, 2009) of CO_2 in ethanolamine takes place (the two chemical elements circulating in counter current), resulting the carbamate in the lower part of A (pipe 3) and a gas phase (containing CO_2 at a concentration lower than 0.1%) in its upper part (pipe 4). The carbamate is used to supply the separation column SC through the pipe 3, respectively the gaseous phase is evacuated from the plant through pipe 4. Also, the CO_2 resulted after the carbamate decomposition enters in SC through the pipe 7, in this system element the chemical exchange between the carbamate and CO_2 taking place (in SC the two mentioned chemical elements circulate in counter-current, too). During the chemical exchange process, the enrichment of

the ^{13}C isotope is accomplished, it concentrating in liquid phase in the lower part of the SC (Axente et. al, 1994). The most important parameter which has to be monitored and controlled is the ^{13}C isotope concentration. The concentration value can be measured using the concentration transducer (mass spectrometer) T placed on the pipe 2 at the output from SC. Through the pipe 2, the carbamate is sent to the reactor R, where the thermal decomposition of this solution is made. The resulted CO_2 (with a higher concentration of the ^{13}C isotope comparing with the initial conditions values) is returned to the SC through the pipe 7. Also, the CO_2 is completely removed after the stripping procedure (in the stripper S), resulting the ethanolamine. The ethanolamine is reheated in the heater H and circulated again through the plant using the pump P and the pipe 1. The CO_2 quantity which passes through the SC is sent to the absorber through the pipe 5.

In production regime, the pipe 6 is used to supply the plant with CO_2 , the product being extracted in gaseous phase (CO_2 with a certain concentration of ^{13}C through the pipe 8). Obviously, in production

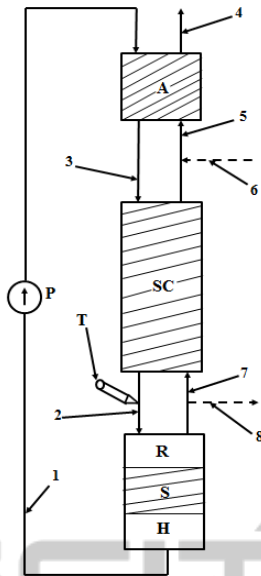


Figure 1: The separation plant.

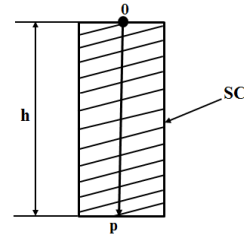
regime, some connecting pipes are used to connect pipes 6 and 8. In Figure 1, the hatched zones signify that the corresponding elements present steel pack of Helipack type. The steel pack has a determinant contribution in the plant working, making possible the ^{13}C isotope separation (Axente et. all, 1994).

The problem of ^{13}C separation is treated in a few papers from the technical literature, for example in (Li et. all, 2010), but the proposed solutions for improving the separation process are not based on using an advanced control strategy. Also, all the control solutions are referring only to the ^{13}C isotope concentration control at the base of SC (associated to the position of T from Figure 1). At this moment, the treated separation plant is controlled using an on-off concentration controller which does not ensure the necessary control accuracy and it introduces undesired fluctuations in the system.

2 PROCESS MODELING

The ^{13}C isotope separation process is a distributed parameter process (Li and Qi, 2011), the output signal y (the ^{13}C concentration) depending both on the independent variable time (t) and on the position in the SC in relation to its height. The concentration variation in relation to the position in the transversal section of SC is insignificant and it is not considered in the process model. In order to highlight the second independent variable “length” notated with p , the $0p$ axis from Figure 2 is defined. The origin 0 of the $0p$ axis is the centre of the transversal section of

the SC from its upper part (the term transversal section is referring to a section on which the height direction (for example the $0p$ axis) is a vertical line).


 Figure 2: The $0p$ axis.

Due to the fact that SC has a cylindrical form, each transversal section is a circle. The diameter of the transversal section is $d = 2.5\text{cm}$ and the column height is $h = 300\text{cm}$ (Axente et. all, 1994). Considering the previous aspects, the p independent variable has the definition domain $p \in \{[p_0, p_f] = [0, h]\}$. The $y(t,p)$ signal has an increasing evolution in relation to the both independent variables, implying that the approximating analytical solution which describes the process work in transitory regime contains two functional terms that have to be determined, one in relation to t ($F_t(t)$) and the second one in relation to p ($F_p(p)$). The modelling procedure is valid for all working regimes, but only after the CO_2 enters the first time in the SC through the pipe 8. First, the expression of the $F_t(t)$ function is determined. The height equivalent to a theoretical plate (HETP) is a function depending on the input ethanolamine flow. Knowing that the dependence between HETP and ethanolamine input flow F_{in} is a linear one (Axente et. all, 1994), the following relation can be written:

$$\text{HETP}(t) = \text{HETP}_0 + K_H \cdot (F_{in}(t) - F_{in0}), \quad (1)$$

where $\text{HETP}(t)$ is the instantaneous value of the height of the equivalent plate, HETP_0 is the steady state value of the height of the equivalent plate for the ethanolamine input flow $F_{in0} = \text{ct.}$, K_H is a proportionality constant which makes the connection between the ethanolamine input flow and HETP and $F_{in}(t)$ is the instantaneous value of the ethanolamine input flow. The proportionality constant K_H is determined using some experimental data resulted from the plant. Each experiment is made measuring the evolution in time of the output signal $y(t,p)$ for different step type variations of the input signal $F_{in}(t)$. The value of the reference input flow is chosen from the experimental data $F_{in0} = 367\text{ml/h}$, its corresponding HETP_0 having the value 4.64cm .

In (Axente et. all, 1994) it was proved that K_H is the gradient of the ramp resulted after the graphical

representation of the function $HETP_{st}(F_{in})$, where $HETP_{st}$ represents the steady state values of HETP corresponding to different F_{in} step signals. Determining, also experimentally, that for $F_{in1} = 460\text{ml}$, $HETP_{st1} = 5.43$, K_H can be computed using the relation:

$$K_H = \frac{HETP_{st1} - HETP_0}{F_{in1} - F_{in0}}, \quad (2)$$

resulting after computation $K_H = 0.0085(\text{cm}\cdot\text{h})/\text{ml}$.

The instantaneous value of the number of the theoretical plates is given by:

$$n(t) = h/HETP(t). \quad (3)$$

Also, the isotope separation can be computed using relation (4):

$$S(t) = \alpha^{n(t)}, \quad (4)$$

where $\alpha = 1.01$ is the elementary separation factor of the ^{13}C isotope for the carbamate – CO_2 chemical exchange procedure. Considering (1), the positive value obtained for K_H constant implies the increase of $HETP(t)$ at the increase of $F_{in}(t)$. Also, from (3) and (4) the decrease of the number of theoretical plates, respectively of the isotope separation value, results. The main consequence of the last two remarks is the fact that the $y(t,p)$ signal decreases at the $F_{in}(t)$ increasing, respectively the $y(t,p)$ signal increases at the $F_{in}(t)$ decreasing. From the physical point of view, this phenomenon is explained due to the fact that lower the value of the input ethanolamine flow $F_{in}(t)$ is, the longer the contact duration between the carbamate and CO_2 in SC is, the chemical exchange between the two chemical elements being a more efficient one.

Also, the isotope separation is given by the relation:

$$S(t) = \frac{y(t_f, p_f)(F_{in}(t))}{y_0}, \quad (5)$$

where $y_0 = 1.108\%$ represents the natural abundance of the ^{13}C isotope and $y(t_f, p_f)(t)$ is the steady state value of the output signal for a certain input step type signal which would have the instantaneous value of the signal $F_{in}(t)$, considering that $p = p_f = 300\text{cm}$. From (4) and (5), it results that:

$$y(t_f, p_f)(F_{in}(t)) = y_0 \cdot \alpha^{n(t)}, \quad (6)$$

or

$$y(t_f, p_f)(F_{in}(t)) = y_0 \cdot S(t). \quad (7)$$

The ^{13}C concentration increase over the initial value y_0 , in steady state regime, is given by:

$$y(t_f, p_f)(F_{in}(t)) - y_0 = y_0 \cdot (\alpha^{n(t)} - 1) = y_0 \cdot (S(t) - 1). \quad (8)$$

The final input signal in the process is defined by:

$$u_f(t) = y_0 \cdot (S(t) - 1). \quad (9)$$

Obviously, if $F_{in}(t)$ is a step type signal it results that the $u_f(t)$ signal is a step type signal, too.

The isotope separation process is a first order one, being characterized by only one time constant. The time constant of the process is experimentally determined and if the experiment based on a step type variation of the input signal $F_{in}(t)$ is made for $p = p_f$, it can be determined using the tangent method, resulting the value $T_{pf} = 14\text{h}$. If the same experiment is repeated, but the measurement of the output signal $y(t,p)$ is made in the close neighbourhood of the origin 0 on the $0p$ axis (for the value $p = 0^+$), after applying the tangent method, it results for the process time constant the value $T_{p0} = 2\text{h}$.

From these experimental identifications of the two time constants, it results that the process time constant increases progressively from the upper part to the lower part of SC along the $0p$ axis. Next, in this paper, a linear increasing evolution of the T time constant of the process along the $0p$ axis is considered, given by the relation:

$$T = T_{p0} + (T_{pf} - T_{p0}) \cdot \frac{p}{p_f}, \quad (10)$$

where $p_f = h$. From (10) it can be remarked that $T = T(p)$, but the changing of the value of the p independent variable is not made continuously. The p value changing is made at discrete time moments through the changing of the transducer T position inside the SC along the $0p$ axis. The commutations of the p independent variable can be viewed as step type signals.

The first order differential equation which describes the relation between the final input signal $u_f(t)$ and the function $F_t(t)$ ($F_t(t)$ being the solution of this equation) is:

$$\frac{dF_t(t)}{dt} = -\frac{1}{T(p)} \cdot F_t(t) + \frac{1}{T(p)} \cdot u_f(t). \quad (11)$$

In the previous equation, the p independent variable change implies the value changing of the process time constant $T(p)$, the effect of such a variation influencing the $F_t(t)$ function only in transitory regime. Consequently, F_t depends on both independent variable $F_t(t,p)$ only in the commutation moments of the p independent variable and only

when this commutation takes place in transitory regime. Also, the $F_t(t)$ function represents the ^{13}C concentration evolution in time over the value y_0 until the value $y(t_f, p_f)$ for a certain value of $F_{in}(t)$. If the value of the p variable is changed, the speed evolution of the $F_t(t)$ function is adapted, but its steady state value remains at $y(t_f, p_f)$. This problem is solved introducing in the approximating analytical solution the $F_p(p)$ function.

The $F_p(p)$ function can be determined in two stages. Firstly, the $F_{p1}(p)$ function is determined. The $y(t, p)$ evolution in relation to the p independent variable for $t = t_f$ and for a certain constant value of the F_{in} signal is given by the relation:

$$y(t_f, p) = y_0 \cdot \alpha^{n(t_f)}, \quad (12)$$

As it results from (12), the evolution in time of the $y(t_f, p_f)$ signal has a hyperbolic form. Using a mathematical procedure based on an interpolation method, the $y(t_f, p)$ signal can be approximated by a $F_{p1}(p)$ function of the form:

$$F_{p1}(p) = (y_0 \cdot \alpha - 1) + e^{\frac{p}{430 + K_p \cdot (F_{in}(t) - F_{in0})}}, \quad (13)$$

where $C = 430\text{cm}$ is a SC constant determined through interpolation and $K_p = 0.7527(\text{cm} \cdot \text{h})/\text{ml}$ results using two consecutive determined sets of values $\{F_{in}, P\}$. The "length" constant P is:

$$P = 430 + K_p \cdot (F_{in}(t) - F_{in0}). \quad (14)$$

As it can be remarked, the $F_{p1}(p)$ function can be modelled using only one "length" constant P . Also, from (14), it results that P is a function of the input ethanolamine flow $P(F_{in}(t))$, implicitly a function of time $P(t)$. It results that F_{p1} is a function depending on $F_{in}(t)$ ($F_{p1}(F_{in}(t), p)$) and implicitly on both independent variables t and p ($F_{p1}(t, p)$).

Secondly, the function $F_{p2} = F_{p1}(F_{in}(t), p_f)$ is determined. The final form of the $F_p(p)$ function results using the relation:

$$\begin{aligned} F_p(p, F_{in}(t)) &= \frac{F_{p1}(F_{in}(t), p) - y_0}{F_{p2} - y_0} = \\ &= \frac{F_{p1}(F_{in}(t), p) - y_0}{F_{p1}(F_{in}(t), p_f) - y_0}, \end{aligned} \quad (15)$$

this function depending on the input flow $F_{in}(t)$, too.

Also, the final form of the approximating analytical solution is given by:

$$y_{AN}(t, p) = y_0 + F_t(t) \cdot F_p(p, F_{in}(t)). \quad (16)$$

Due to the facts that, $F_p = F_p(F_{in}(t), p)$, it results as ratio between two other functions ($(F_{p1} - y_0)$ and $(F_{p2} - y_0)$) and for some particular cases $F_t = F_t(t, p)$, getting to the conclusion that the treated separation

process is a strong non-linear one.

3 LEARNING THE PROCESS BEHAVIOUR USING NEURAL NETWORKS

The approximating analytical solution from (16) which describes the working of the separation process, the process being a distributed parameter one (Smyshlyaev and Krstic, 2005), has a very complex structure. Considering this aspect, the analytical solution is decomposed in some more simple mathematical components. Each resulted mathematical component is modelled using a neural network and, after that, in order to obtain the model of the entire analytical solution, the resulted neural networks are properly interconnected between them.

The two types of neural structures used to learn (Borges, 2011) the behaviour of the components of the analytical solution are the forward fully connected neural networks and the autoregressive fully connected networks with exogenous inputs (Haykin, 2009). The two types of neural networks are presented schematically in Figures 3 and 4. In both cases, i_s represents the input signal in the neural network and o_s represents the output signal from the neural network. In all the cases from this paper, the network from Figure 3 contains non-linear neurons in the hidden layer (N_{1i} neurons, where $i = 1, \dots, n$) having hyperbolic tangent activation functions. Also, in all the cases, the N_{21} neuron is linear (having linear activation function (Maren et. all, 1990; Norgaard et. all, 2000)).

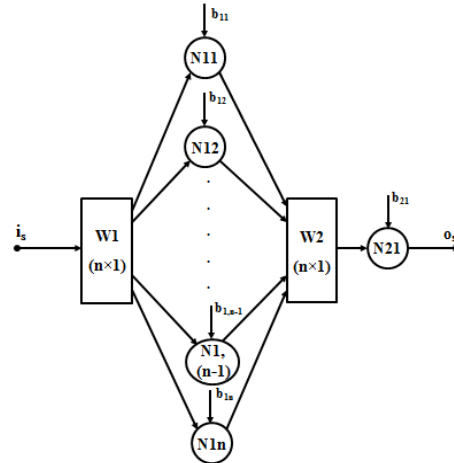


Figure 3: The forward fully connected network.

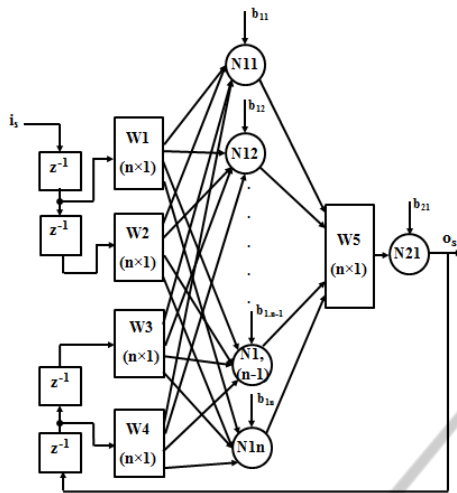


Figure 4: The autoregressive fully connected network with exogenous inputs.

The $W1$ and $W2$ vectors are column vectors containing the weights that make the connection between the input layer and the hidden layer, respectively between the hidden layer and the output layer. The n dimension (the dimension of the hidden layer) can be singularized for each application in part. The output signal o_s , for the general structure from Figure 3 is given by the relation:

$$o_s = [\tanh(i_s \cdot W1^T + B1^T) \cdot W2 + b21], \quad (17)$$

where $B1$ is a column vector containing the bias values of the neurons from the hidden layer, $b21$ is the bias value of the $N21$ neuron, the superscript T signifies that the corresponding vector is considered in transposed form and the notation “tanh” signifies the application of the hyperbolic tangent functions to all the elements of the corresponding vector.

The structure from Figure 4 is used in the case when the work of the components is expressed using differential equations. The elements z^{-1} represent delay lines used both on the input and on the feedback signal, in order to memorize the previous values of the two signals. The connection between the input layer (formed by the input signal and the feedback signal) and the hidden layer is made through the column vectors $W1$ and $W2$, respectively $W3$ and $W4$, all of them containing weights. $W5$ has the same significance as $W2$ in the case of Figure 3 and the dimension n is singularized, also, for each application in part. In the case of the network from Figure 4, all the neurons are linear. The o_s signal is given by the relation:

$$o_s(k) = [W1^T \cdot i_s(k-1) + W2^T \cdot i_s(k-2) + W3^T \cdot o_s(k-2) + W4^T \cdot o_s(k-1) + B1^T] \cdot W5 + b21, \quad (18)$$

where $B1$, $b21$ and T have the same significance as in the case of relation (17), respectively the sequence (k) represents the current value of the signals, and the sequences $(k-1)$ and $(k-2)$ represent the previous two values of the signals. If only one unit line is necessary for a certain application both on the input and on the feedback signals, the same presented structure can be used considering the elements of the matrices $W2$ and $W3$ equal to 0 (Vălean, 1996).

The implementation of the approximating analytical solution from (16) using neural networks is presented in Figure 5. The neural networks noted with NN are trained in order to learn the functional dependence between the corresponding input and output signals. Practically, the neural structure from Figure 5 resulted following the relations (1)-(16) and interconnecting the component neural networks, obviously processing mathematically the signals that occur in the structure. All the neural networks from Figure 5, instead of NN4 are forward fully connected ones with $n = 10$. They are trained using 1000 input-output data pairs and considering, also, a ramp type variation of the corresponding input signals. In all cases, as training algorithm, the Levenberg-Marquardt back-propagation algorithm is used. The maximum number of training epochs was fixed to 20000, obtaining in all cases very small error values (values proportional with 10^{-13} ; the quality indicator is considered the mean square error). The neural network NN4 implements the integration function.

In this case the autoregressive fully connected network with exogenous inputs structure from Figure 4 is used, considering all the elements of the vectors $W2$ and $W3$ equal to 0 (only 1 unit delay both on the input and on the output signals). Also, in this case $n = 7$. The same number of input-output data pairs and the same training algorithm are considered as in the case of the other Neural Networks from Figure 5, but a white noise variation of the input signal. The imposed value of the mean square error is reached after 15 training epochs. The neural model implemented in Figure 5 and associated to the analytical solution from (16) will be used as the process Reference Model in the IMC control structure.

4 THE PROPOSED CONTROL STRUCTURE

The control structure based on the Internal Model Control (IMC) strategy (Love, 2007; Golnaraghi et.

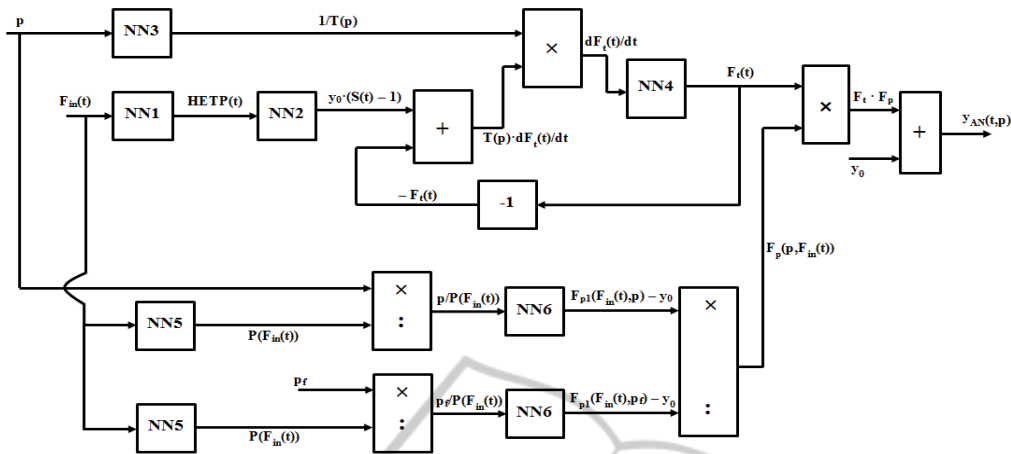


Figure 5: The implementation of the approximating analytical solution using neural networks.

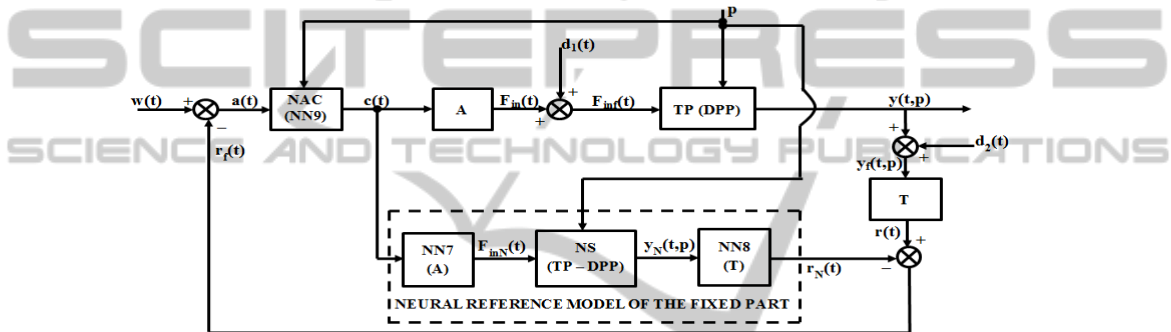


Figure 6: The proposed IMC structure.

all, 2009), proposed to be used for the concentration control of the ¹³C isotope, is presented in Figure 6.

The elements from the direct physical channel of the structure are: the actuator A (the pump P from Figure 1), the distributed parameter (DPP) technological process (TP) and the transducer T (the same transducer as in Figure 1). Also, the elements from the direct reference channel represent the neural networks that describe the work of the elements from the physical direct channel: NN7 for A, NS (neural structure from Figure 5) for the TP (DPP) and NN8 for T. The three neural models connected in series represent the Neural Reference Model of the Fixed Part of the system. Also the element NAC is the Neural Adaptive Controller modelled using the neural structure NN9. From the mathematical point of view, the NAC controller is a distributed parameter controller. The term “distributed parameter controller” is referring to the fact that one of the controller parameters (the main parameter) depends on the value of the p independent variable. This term does not have the meaning of a spatial distribution of the generated control signal. Also the significance of the notations

regarding the signals from Figure 6 is: $w(t)$ – reference signal, $c(t)$ – control signal, $F_{in}(t)$ – actuating signal (the input flow of ethanolamine), $d_1(t)$ – disturbance signal which affects directly the actuating signal, $F_{inr}(t)$ – disturbed actuating signal (the final value of the ethanolamine input flow), $y(t, p)$ – output signal (the ¹³C isotope concentration), $d_2(t)$ – disturbance signal which affects directly the output signal, $y_f(t, p)$ – disturbed output signal due to the effect of $d_2(t)$, respectively $r(t)$ – feedback signal.

Also, the $F_{inN}(t)$, $y_N(t, p)$, and $r_N(t)$ signals have the same significance as the signals $F_{in}(t)$, $y(t, p)$ and $r(t)$, but represent output signals from the corresponding elements of the Reference Model of the Fixed Part. These signals are not disturbed, the disturbances not affecting the reference direct channel of the system. The final feedback signal $r_f(t) = r(t) - r_N(t)$ represents a measure of all disturbances effects that affect in a negative manner the work of the physical direct channel ($d_1(t)$, $d_2(t)$, but also the parametric disturbances (variations in time of the parameters of the elements A, TP and T)). Also $a(t) = w(t) - r_f(t)$ is the error signal. It can be remarked that the value of the p independent

variable is transmitted to both direct channels and to the controller.

The structure from Figure 6 can work, in the case the p variable value is not transmitted to the reference direct channel, but this case is not treated in this paper. Also, the structure can be adapted for the case when the automatic determination of the p value is necessary (Muresan and Abrudean, 2010), case which also, is not treated in this paper. The work of the actuator A, it having a linear behaviour, is expressed using a second order transfer function. The values of the time constants of the actuator are: $T_A = 0.1\text{min}$ (the time constant of the actuator) and $T_1 = 2\text{min}$ (the time constant introduced using an electronic equipment in order to “delay” the propagation of the control signal to the actuator). Also, the proportionality constant of the actuator $K_A = -56.25\text{ ml/(h}\cdot\text{mA)}$. The generated output signal represents the value of the ethanolamine flow which has to be subtracted from F_{inmax} in order to obtain the F_{in} signal. This adjustment is necessary due to the fact that the plant technological start is made using F_{inmax} . The A element is modelled using the neural network 7 (NN7). NN7 has exactly the structure from Figure 4, for $n = 10$. Also all the delay lines from Figure 4 are necessary due to the fact that the actuator model is of second order. The network NN7 is trained using the same training algorithm as in the case of NN4, the same type of input signal and 500 pairs of input-output data. The imposed mean square error of is reached after 17 training epochs. The used sampling time, in this case, has the value $T_s = 0.036\text{ min}$. This value is much smaller than the value of the sampling time used for the training of all neural networks from the previous Paragraph (3) ($T_s = 30\text{ min}$) due to the much smaller time constants values of the actuator comparing to the value of the time constant of the technological process.

The transducer T model is expressed using a first order transfer function with $K_T = 5.7143\text{mA}/\%$ (the proportionality constant of the transducer) and $T_T = 6\text{min}$ (the time constant of the transducer). The computation of K_A and K_T proportionality constants is made taking in consideration the fact that the automation equipment used for this application works with unified current signals. This model is learned using the NN8 neural network from Figure 6. The network parameters and the training parameters are the same as in the case of the NN4 training, with the exception that $T_s = 0.09\text{min}$.

The controller is tuned in order to compensate the main time constant of the process $T(T(p))$. The mathematical model which describes the controller work in time domain is expressed using the

following differential equation:

$$T_f \cdot \frac{dc(t)}{dt} + c(t) = T(p) \cdot \frac{da(t)}{dt} + a(t), \quad (19)$$

where T_f is the time constant of the first order filter used in order to obtain the controller feasibility ($T_f < T(p)$). The control signal $c(t)$ represents the solution of the equation (19). At the changing of the p independent variable value, the value of the process time constant is modified and from (19) it results that the value of the $T(p)$ time constant of the controller is modified, too, in order to be adapted to the new time constant of the process. This explanation implies the term “adaptive controller”. Also the modification of the $T(p)$ value is made through the value of p independent variable, being justified the abstract term of “distributed parameter controller”. The implementation of the controller using three neural networks interconnected between them using mathematical operators, is presented in Figure 7. The NN31 has the same structure as NN3 from Figure 5, generating at the output the value $T(p)$. Also, the NN41 structures have the same structure as NN4 from Figure 5, implementing the integration operation. The training procedures and parameters for the two types of neural networks from Figure 7 are the same as in the case of NN3 and NN4 from Figure 5, with the exception of the sampling time (in this case $T_s = 3\text{min}$). In the case when the ^{13}C isotope concentration control is made in the point $p = p_f$, the value $T_f = 8\text{h}$ represents a good compromise between the system stability and the structure performances. Also, for this value, the usage of the control signal is feasible from its saturation values avoidance point of view.

Having the neural models of the elements A, TP and T, practically the model of the Reference Model of the Fixed Part can be implemented, for example, on a process computer and the structure from Figure 6 can be used. The model of the controller, also expressed using a neural networks structure, can be implemented on a computation equipment, too.

5 SIMULATION RESULTS

The simulations (Colosi et. all, 2013) are made in MATLAB/Simulink. First the validity of the analytical solution from (16) is verified. In Figure 8 is presented the comparative graph between 5 step responses of the separation column model expressed through the mentioned analytical solution, if the simulation is made for $p = p_f$. The values of the considered input step type variations are $F_{\text{in}} \in \{200;$

280; 367; 416; 600}ml/h. The steady state values of the ¹³C concentration isotope ($y(t_r, p_f)$) are centralized in Table 1.

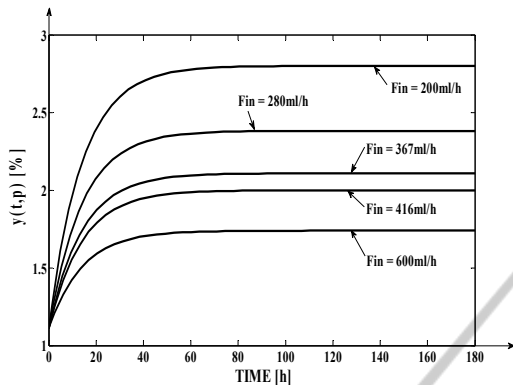


Figure 8: Open loop responses of the determined process model for different values of the input signal.

Table 1: The simulation results associated to Figure 8.

| F_{in} [ml/h] | $y(t_r, p_f)$ [%] |
|-----------------|-------------------|
| 200 | 2.8 |
| 280 | 2.3818 |
| 367 | 2.1083 |
| 416 | 2 |
| 600 | 1.7392 |

Comparing to the experimental data from (Axente et. all, 1994), it results that the determined approximating analytical solution describes the process work with high accuracy, the differences occurring only at the third decimal. Also, in Table 1 and Figure 8 the increasing evolution of the ¹³C isotope concentration at the decrease of the value of the input ethanolamine flow is highlighted.

In Figure 9 is presented the comparative graph between 4 step responses of the separation column model expressed through the mentioned analytical solution, if the input flow of ethanolamine presents a step type variation with the value $F_{in} = 300$ ml/h, for different values of the p independent variable

$p \in \{p_f/4; p_f/2; p_f/4 \cdot 3; p_f\}$ [cm]. The steady state values of the ¹³C isotope concentration ($y(t_r, p)$) from Figure 9 are centralized in Table 2.

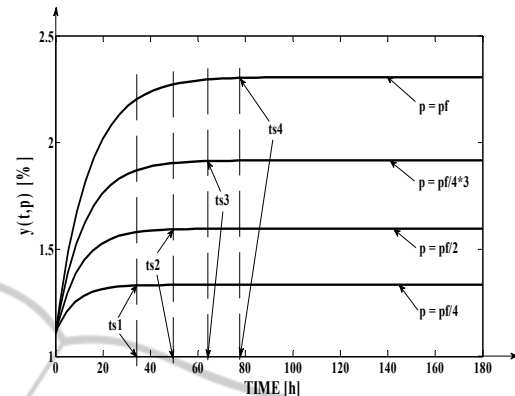


Figure 9: Open loop responses of the determined process model for different values of the p independent variable.

Table 2: The simulation results associated to Figure 9.

| p [cm] | $y(t_r, p)$ [%] |
|-----------------|-----------------|
| $p_f/4$ | 1.3345 |
| $p_f/2$ | 1.5971 |
| $p_f/4 \cdot 3$ | 1.917 |
| p_f | 2.3069 |

From Figure 9 and Table 2, the decreasing evolution of the process response in relation to the decrease of the p independent variable is highlighted. From the mathematical point of view, this aspect is explained due to the increasing evolution of the F_p function in relation to the increase of p . From the physical point of view, this aspect is explained due to the increase evolution of the number of the theoretical plates in relation to the increase of p . Also, from Figure 9 it can be remarked that lower the value of p is, lower the value of the process settling time is ($t_{s1} < t_{s2} < t_{s3} < t_{s4}$). This phenomenon is explained due to the decreasing evolution of the $T(p)$ process time constant at the decrease of p .

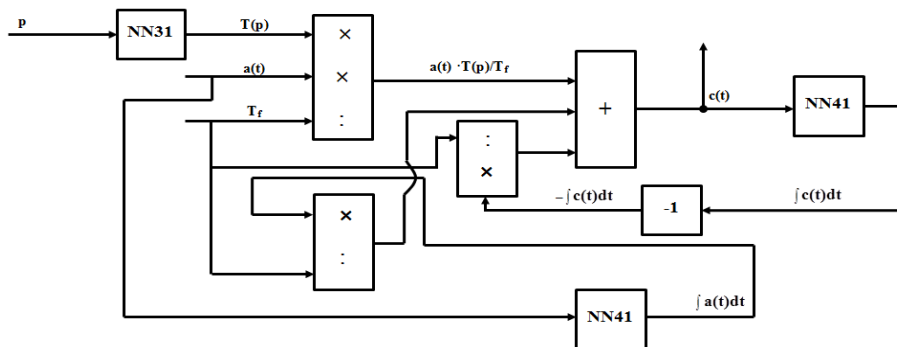


Figure 7: The implementation of the controller using neural networks.

In Figure 10, the comparative graph between the process response (modelled through the analytical solution) and the process response (modelled through the neural structure implemented in Figure 5) is presented. Practically, the differences between the two curves from Figure 10 cannot be distinguished, resulting the high validity of the Neural Reference Model of the Fixed Part of the control system from Figure 6 (the NS element from the Reference Model has the main weight in it). The square mean error between the two curves from Figure 10, computed for 453 pairs of values associated to the two responses, has the value $E_{mp} = 0.0023\%$, considered insignificant for this application.

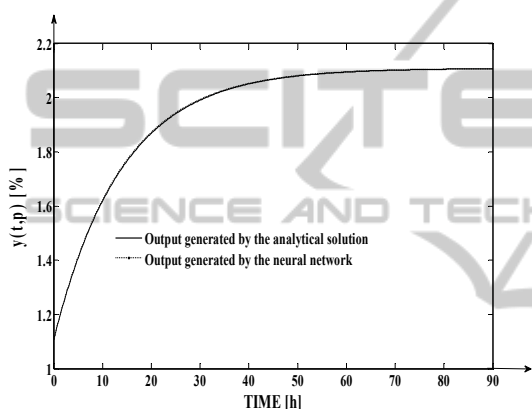


Figure 10: The validation of the neural model associated to the technological process.

In Figure 11, the response of the control system from Figure 6 is presented. Firstly, between the time moments $t_1 = 30h$ and $t_2 = 120h$, the plant works in starting regime, the ethanolamine flow being maintained at F_{imax} . After the ^{13}C isotope concentration (the output signal) gets steady to the value 1.492%, the structure can be used to assure a certain value of the $y(t,p)$ signal. The simulation from Figure 11 is made for $p = p_f$. After the moment t_2 , the concentration reference is set to the value 1.795%. From the Figure it can be remarked that this value is reached after approximately 40h, much faster than in open loop regime (case of t_{s4} from Figure 9 which has the value approximately equal to 78h). Also it can be remarked that the steady state error $a_{st} = 0\%$ and the overshoot $\sigma = 0\%$ (a very important constrain imposed to the treated type of system).

In Figure 12, the simulation from the Figure 11 is repeated until the time moment $t_3 = 190h$. In this moment the disturbance $d_2(t)$ of step type with the value -0.1% occurs in the system. From Figure 12, it

results that the effect of the disturbance is efficiently rejected by the controller after 50h the concentration value being brought back to the value imposed through the reference signal. In both the cases of the simulations from Figures 11 and 12, the saturation limits of the control respectively of the actuating signals (both the minimum and maximum limits) are not reached, the usage of the controller being feasible.

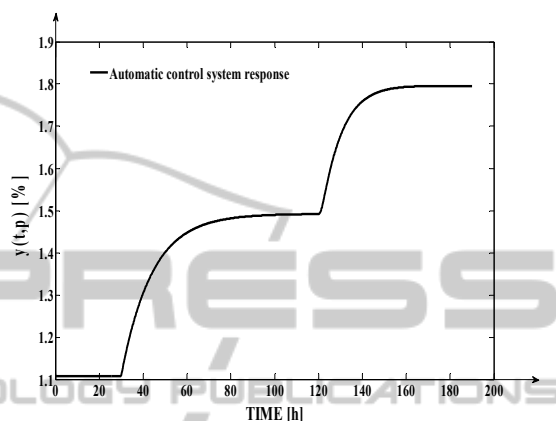


Figure 11: The automatic control system response.

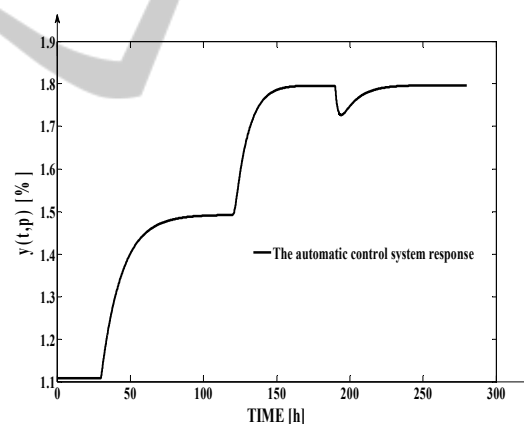


Figure 12: The automatic control system response, for the case when a disturbance signal occurs in the system.

6 CONCLUSIONS

An original solution for the mathematical modelling of a separation technological is presented in this paper. Also, a solution for the automatic control of the ^{13}C isotope concentration is presented based on the IMC strategy.

In order to implement the Reference Model of the system Fixed Part, the neural networks are used.

These elements are original ones, too, due to the fact that a distributed parameter technological process is included in an IMC control structure and the model of this type of process is learned using neural networks. The work of A and T elements (Figure 6) is learned using neural networks in order to preserve the unitary character of the solution and the high accuracy of the Fixed Part mathematical model.

The neural networks are used, also, for implementing the adaptive controller, respectively the term “distributed parameter controller” is introduced and defined.

The process model validity and the high performances of the proposed control structure are proved through the simulations from Paragraph 5. The control structure is tested in the case when a disturbance signal occurs in the system. As it can be remarked from Figure 12, the effect of the disturbance is rejected with high efficiency.

ACKNOWLEDGEMENTS

The research activity that helped the authors to elaborate the paper is supported through the research projects no. 30141/12.12.2014 and no. 30104/2014, financed by the Technical University of Cluj-Napoca.

REFERENCES

- Axente, D., Abrudean, M., Bâldea, A., 1994. ^{15}N , ^{18}O , ^{10}B , ^{13}C Isotopes Separation through Isotopic Exchange, Science Book House.
- Borges, R. V., 2011. Learning and Representing Temporal Knowledge in Recurrent Networks. In *IEEE Transactions on Neural Networks*, Vol. 22, Issue 12, pp. 2409 – 2421.
- Coloși, T., Abrudean, M., Ungureșan, M.-L., Mureșan, V., 2013. *Numerical Simulation of Distributed Parameter Processes*, Springer.
- Dang, H., Rochelle, G. T., 2003. CO_2 absorption rate and solubility in monoethanolamine/ piperazine/ water. In *Separation Sci. & Tech.*, Vol. 38 (2), pp. 337–357.
- Dugas, R., Rochelle, G., 2009. Absorption and desorption rates of carbon dioxide with monoethanolamine and piperazine. In *Energy Procedia*, Vol. 1 (1), pp. 1163–1169.
- Golnaraghi, F., Kuo, B. C., 2009. *Automatic Control Systems, 9th edition*, Wiley Publishing House.
- Haykin, S., 2009. *Neural Networks and Learning Machines, Third Edition*, Pearson Int. Edition.
- Li, H.-L., Ju, Y.-L., Li, L.-J., Xu D.-G., 2010. Separation of isotope ^{13}C using high-performance structured packing. In *Chemical Engineering and Processing: Process Intensification*, Vol. 49 (3), pp. 255–261.
- Li, H.-X., Qi, C., 2011. *Spatio-Temporal Modeling of Nonlinear Distributed Parameter Systems: A Time/Space Separation Based Approach, 1st Edition*, Springer.
- Love, J., 2007. *Process Automation Handbook, 1 edition*, Springer.
- Maren, A., Harston, C., Pap, R., 1990. *Handbook of Neural Computing Applications*, Academic Press.
- Mureșan, V., Abrudean, M., 2010. Temperature Modelling and Simulation in the Furnace with Rotary Hearth. In *Proc. of IEEE AQTR-17th ed.*, Cluj-Napoca, Romania, pp. 147-152.
- Norgaard, M., Ravn, O., Poulsen, N.K., Hansen, L.K., 2000. *Neural Networks for Modelling and Control of Dynamics Systems*, Springer.
- Smyshlyaev, A., Krstic, M., 2005. Control design for PDEs with space-dependent diffusivity and time-dependent reactivity. In *Automatica*, Vol. 41, pp. 1601-1608.
- Vălean H., 1996. Neural Network for System Identification and Modelling. In *Proc. of Automatic Control and Testing Conference*, Cluj-Napoca, Romania, 23-24 May, pp. 263-268.